NEUROSCIENCE

Spatial representations of self and other in the hippocampus

Teruko Danjo,[1] Taro Toyoizumi,[2] Shigeyoshi Fujisawa[1]*

An animal's awareness of its location in space depends on the activity of place cells in the hippocampus. How the brain encodes the spatial position of others has not yet been identified. We investigated neuronal representations of other animals' locations in the dorsal CA1 region of the hippocampus with an observational T-maze task in which one rat was required to observe another rat's trajectory to successfully retrieve a reward. Information reflecting the spatial location of both the self and the other was jointly and discretely encoded by CA1 pyramidal cells in the observer rat. A subset of CA1 pyramidal cells exhibited spatial receptive fields that were identical for the self and the other. These findings demonstrate that hippocampal spatial representations include dimensions for both self and nonself.

Spatial navigation requires the hippocampus (*1*, *2*). The cognitive map theory states that spatial recognition in the hippocampus is allocentric (*3*–*5*). Place cells in the hippocampus are the physiological correlate of this representation because they are highly sensitive to changes in landmarks and contexts (*6*–*13*). The characterization of additional types of navigational representations, including head-direction cells and grid cells, has promoted our understanding of the neural mechanisms of allocentric spatial representations in the hippocampal-entorhinal cortex network (*14*–*19*). The studies of these neural maps have focused on the animal's own position in space. It still remains unclear whether and how spatial information of nonself, such as the position of conspecifics, landmarks, and moving objects, is represented in the hippocampus.

We designed an observational T-maze task using a pair of rats (hereafter termed "self" and "other") and investigated how the other's position is represented in the self's hippocampus. The self was required to make a left/right choice to retrieve a reward based on the location of the other. We used two versions of the task, an "opposite-side rule" version in which the self rat had to choose the side opposite to the other's location (Fig. 1A, fig. S1, and movie S1) and a "same-side rule" in which the self rat had to choose the same side as the other rat (fig. S1 and movie S2). During the T-maze task, neuronal activity in the self's hippocampus (dorsal CA1) was recorded extracellularly (n = 3 pairs of rats; 88 ± 8.1% and 84 ± 11% correct performance with opposite-side and same-side rules, respectively). All analyses were performed on single units with pyramidal cell features and place fields in the task area (n = 1298 and 1205 units with opposite-side and same-side rules, respectively) (fig. S2) [see the supplementary materials (SM)].

We first examined how the location of the other rat was represented in the opposite-side rule observational task. Firing-rate maps of the self's positions ("self's rate map") and the other's positions ("other's rate map," which were obtained by replacing the self's positional data with the other's) revealed that in addition to the expected coding of the observer's own position in space, the majority of units also displayed obvious place fields for the other (Fig. 1, C to F, top). To understand the positional relationship of the rat pair at the time of firing, we constructed joint rate maps by linearizing the rats' trajectories and entering them into two-dimensional x-y axes (fig. S3). Here, the self's and other's place fields composed from identical spikes were combined into a single joint place field (Fig. 1, C to F, bottom, and fig. S4). We then examined whether these joint place fields were truly modulated by the other's positions and not a mere consequence of the constraints in the positional relationships of the two rats. The null hypothesis was that the firing only depended on the self's position and was independent of the other's. By computing the surrogate firing rates that followed this null hypothesis (see the SM) (*20*), we identified areas with significantly higher firing rates for the other (P < 0.05) (Fig. 1, C to F, third from top, and fig. S5). A significant firing dependency on the other's positions was detected for 85% of units (Fig. 1, G to I), indicating that the other's spatial information was generally encoded by the place cells in this T-maze task. Importantly, the significant areas were not dependent on the self's specific behavior or the other's positions (Fig. 1, C to I). Moreover, the firing activities of most units were not dependent on the time periods in the trial (fig. S6). Similar results were also observed when we analyzed the same-side rule version of the task (fig. S7).

In the hippocampus, spatial information is encoded not only by the average firing rates of the neurons but also by the timing of the spikes with respect to the phase of the underlying theta oscillations (7 to 11 Hz) (*21*–*24*). We next examined this temporal coding in the other's spatial representations. To control for confounds of the motion of the observer, we focused on units whose rate peaks were located in the self's starting positions in the opposite-side rule and analyzed the relationship between the other's positions and the theta phases of the spikes (n = 78 units). Although the self was not running during the time course of this analysis, the local field potential was dominated by theta oscillations (fig. S8 and SM). In contrast to the lack of theta-phase precession relative to the self's location, 75% of the units displayed significant theta-phase precession as a function of the other's location (P < 0.01) (Fig. 1, J to M). The observed theta-phase precession to the other's location was consistent with that to the self's location, as reported previously (*21*–*24*), demonstrating that the other's spatial information was also temporally encoded in the hippocampal pyramidal cells.

We next sought to dissociate two types of units—those preferentially modulated by the other's position ("other-preferred cells") and those preferentially modulated by the self's goal ["goal-preferred cells," also previously described as "prospective cells" (*25*, *26*)]. We took advantage of the two versions of our observational T-maze task (Fig. 2A). Other-preferred cells fire when the other is located on the same side of the side arms (left or right), irrespective of the rule during a given trial and, as a result, these neurons fire when the self's goal is on a different side across the two conditions (Fig. 2B). This should further support the allocentric representation of the other's place. In contrast, goal-preferred cells increase their firing rate only according to the future choice of the observer. By statistically comparing the other's rate maps between the two versions, we defined other-preferred cells and goal-preferred cells based on these criteria (see the SM). We identified 58 other-preferred cells (Fig. 2, C to G, and fig. S9) and 252 goal-preferred cells (Fig. 2, H and I). Although the number of other-preferred cells was smaller than that of goal-preferred cells, it represented 13% of the place-responsive units examined in this analysis (Fig. 2F and SM), and the firing-rate peaks of both unit groups distributed all along the side arms in the other's rate maps, constituting a full spatial map based on the position of the other rat (Fig. 2, G and I). Furthermore, the analysis of comparing the correct and the error trials in the opposite-side rule resulted in similar percentages of other-preferred and goal-preferred cells (fig. S10).

We next looked for another type of spatial representation, "a common place field" for the self and other, for which a unit fires when either the other or the self is in a specific spatial location. We found 45 units that had common place fields in both the other's and the self's rate maps under the opposite-side rule (Fig. 3, A to E, and SM). We further tested the trajectory specificity of common place fields by separating left- and right-side targeting trials. Notably, we identified 51 of 1244 units in the opposite-side rule task

[1]Laboratory for Systems Neurophysiology, RIKEN Brain Science Institute, 2-1 Hirosawa, Wako, Saitama, 351-0198, Japan. [2]Laboratory for Neural Computation and Adaptation, RIKEN Brain Science Institute, 2-1 Hirosawa, Wako, Saitama, 351-0198, Japan.
*Corresponding author. Email: fujisawa@brain.riken.jp

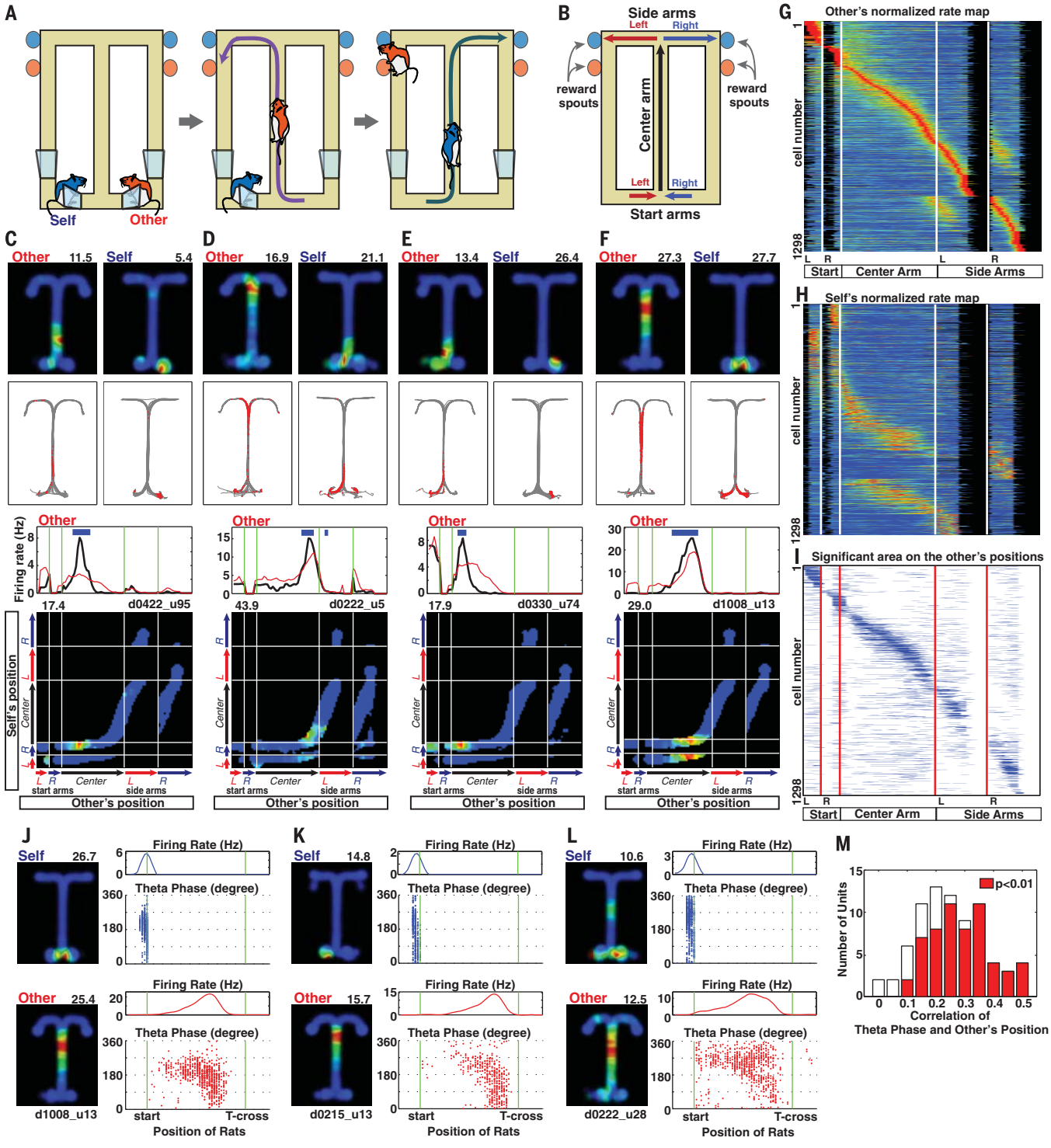

Fig. 1. Joint spatial representations of self and other in the observational task. (**A**) Schematic of the opposite-side rule. See fig. S1A. (**B**) Schematic of linearizing the trajectories on the T-maze. See figs. S3 and S4. (**C** to **F**) Units whose firing rates significantly depended on the other's position. (Top) Other's (left) and self's (right) rate maps. (Second from top) Trajectory plots of other (left) and self (right). Gray lines, rats' trajectories; red dots, spike positions. (Third from top) Linearized rate plots on other's position (black lines). Red lines indicate statistically significant bands ($P < 0.05$) (see fig. S5). Blue thick line indicates the significant area. (Bottom) Joint rate maps. Other's and self's linearized positions are coordinated in horizontal and vertical axes, respectively. The maximum firing rate is indicated at the top of each map. (**G** to **I**) Linearized and normalized rate maps based on the other's position (G), the self's position (H), and the significant area on the other's position (I), sorted by maximum rate positions on the other's map ($n = 1298$ units). (**J** to **L**) Units with theta-phase precession based on the other's position. (Top) Self's rate maps (left), linearized rate plots, and theta phases of the spikes as a function of self's position (right). (Bottom) Other's rate maps (left), linearized rate plots, and theta phases of the spikes as a function of other's position (right). (**M**) Correlation between theta phase and the other's position. Color bars indicate significant correlation ($P < 0.01$; $n = 59$ units).

that had trajectory-specific common place fields (Fig. 3, F and G; fig. S11; and SM), which was significantly higher than the number expected by chance ($P < 0.05$) (see SM).

Because the allocentric representation of self's place was also demonstrated by reliable reconstruction of self's positions only from the spikes of place-cell ensembles (*27*, *28*), we further tested whether the spikes of joint-place-cell ensembles could also reconstruct the other's positions. First, we performed Bayesian decoding analysis with a leave-one-out strategy in each rule (SM). The reconstructed other's trajectories revealed that the spikes of joint-place-cell ensembles contained sufficient information regarding the other's positions (Fig. 4A and fig. S12A). Although the error distances between the actual and decoded positions were larger for the other's decoding than those for the self, the differences in the error distances were as small as 5 cm per time window (200 ms) in both rules (other's versus self's error distances, 20.3 versus 16.1 cm in the opposite-side rule, 20.1 versus 15.1 cm in the same-side rule) (Fig. 4B). We then examined whether these spikes contained more information about the other's place than that obtained by distributions of time spent in the positional relationships of the self and the other. We computed a control estimation of the other's positions by reconstructing the self's positions and then accordingly referring to the probability distributions of the positional relationships (fig. S12B and SM). For the Bayesian reconstructions in this analysis, the prior templates were computed from trials including both rules, and results were examined based on error distances in a block-wise manner

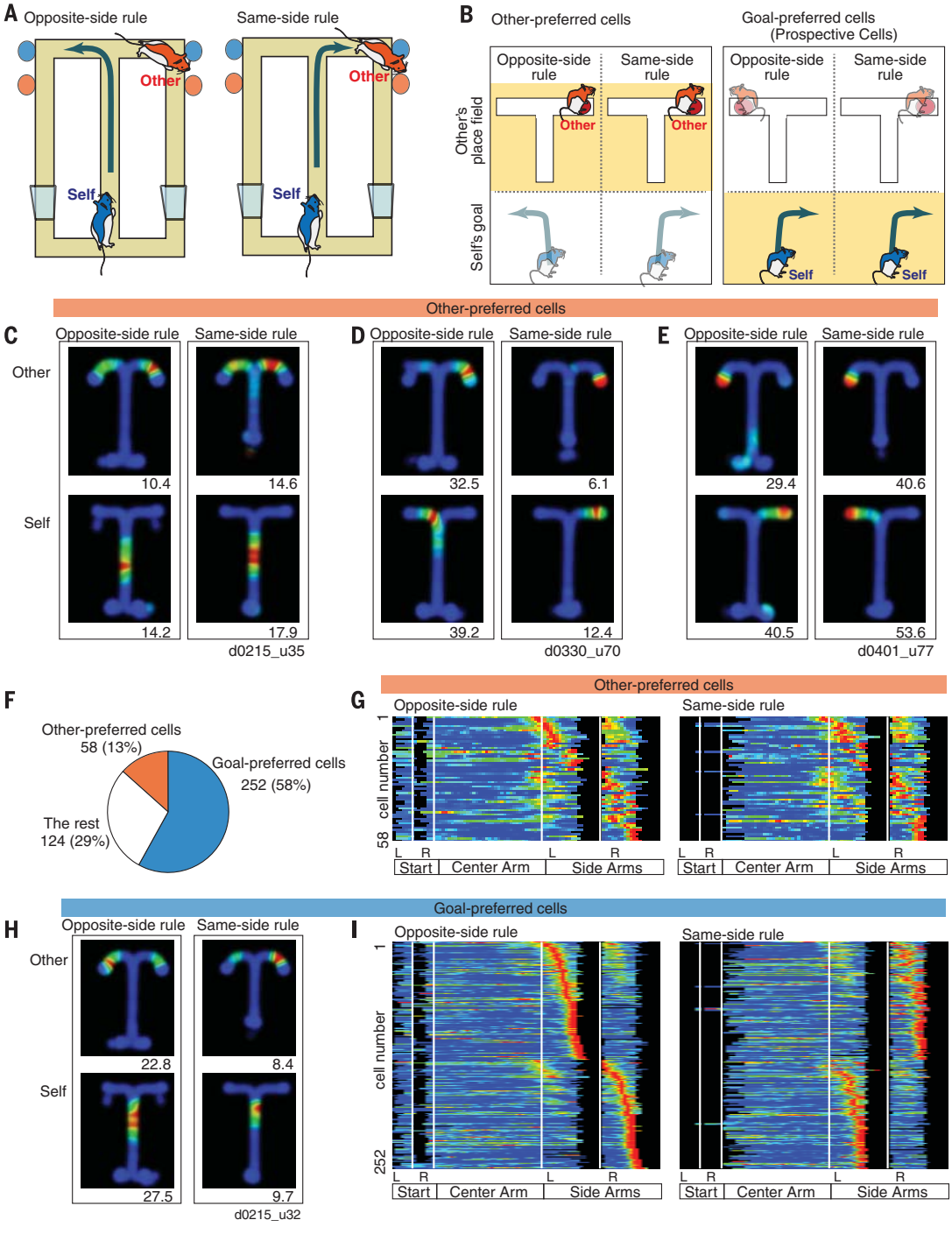

Fig. 2. Spatial representations of other-preferred and goal-preferred cells. (**A**) Schematic of the relationship of the other's position and the self's goal in opposite-side and same-side rules. (**B**) Schematic explaining other-preferred cells (left) and goal-preferred cells (right). Other-preferred cells fire preferentially when the other is on the same side, regardless of the rule. Similarly, goal-preferred cells fire when the self's goal is on the same side. (**C** to **E**) Rate maps of other-preferred cells. (Top) Other's rate maps in the opposite-side rule (left) and same-side rule (right). (Bottom) Self's rate maps in the opposite-side rule (left) and the same-side rule (right). See fig. S9 for statistical methods. (**F**) Summary of other-preferred cells and goal-preferred cells (n = total 434 units). (**G**) Linearized and normalized rate maps of other-referred cells, sorted by peak rate positions. (**H**) Other's (top) and self's (bottom) rate maps of goal-preferred cells in the opposite-side rule (left) and the same-side rule (right). (**I**) Linearized and normalized other's rate maps of goal-preferred cells in the opposite-side task (left) and same-side task (right), sorted by the maximum rate positions.

(Fig. 4, C and D, and SM). Reconstructing trajectories without rule information apparently made the error distances of the other's decoded positions larger, but they were significantly smaller than the control estimate of the other's positions (Fig. 4D). The overall averages of the error distances of the other's decoding were less than 40 cm and also were significantly smaller than those of the control estimation in both rules (Fig. 4E).

We propose an extended model of hippocampal spatial representations that can include dimensions for both self and other (fig. S13). Our model, encompassing various types of spatial representations, can categorize spatial representations into four types: own place fields, joint place fields, other's place fields, and common place fields (fig. S13, A to D). In particular, the common place field could be hypothesized to be a mirror representation of place (*29*, *30*). Combinatorial representations of spatial information of self and nonself would open the door to examining whether this allocentric spatial representation extends more generally to other nonliving moving objects (*31*–*33*) and how it is generated in the hippocampal-entorhinal cortex network. Our data indicate that the place cells in the hippocampus encode sufficient spatial information for organizing the recognition of other animals, which is essential for social behavior (*34*, *35*).

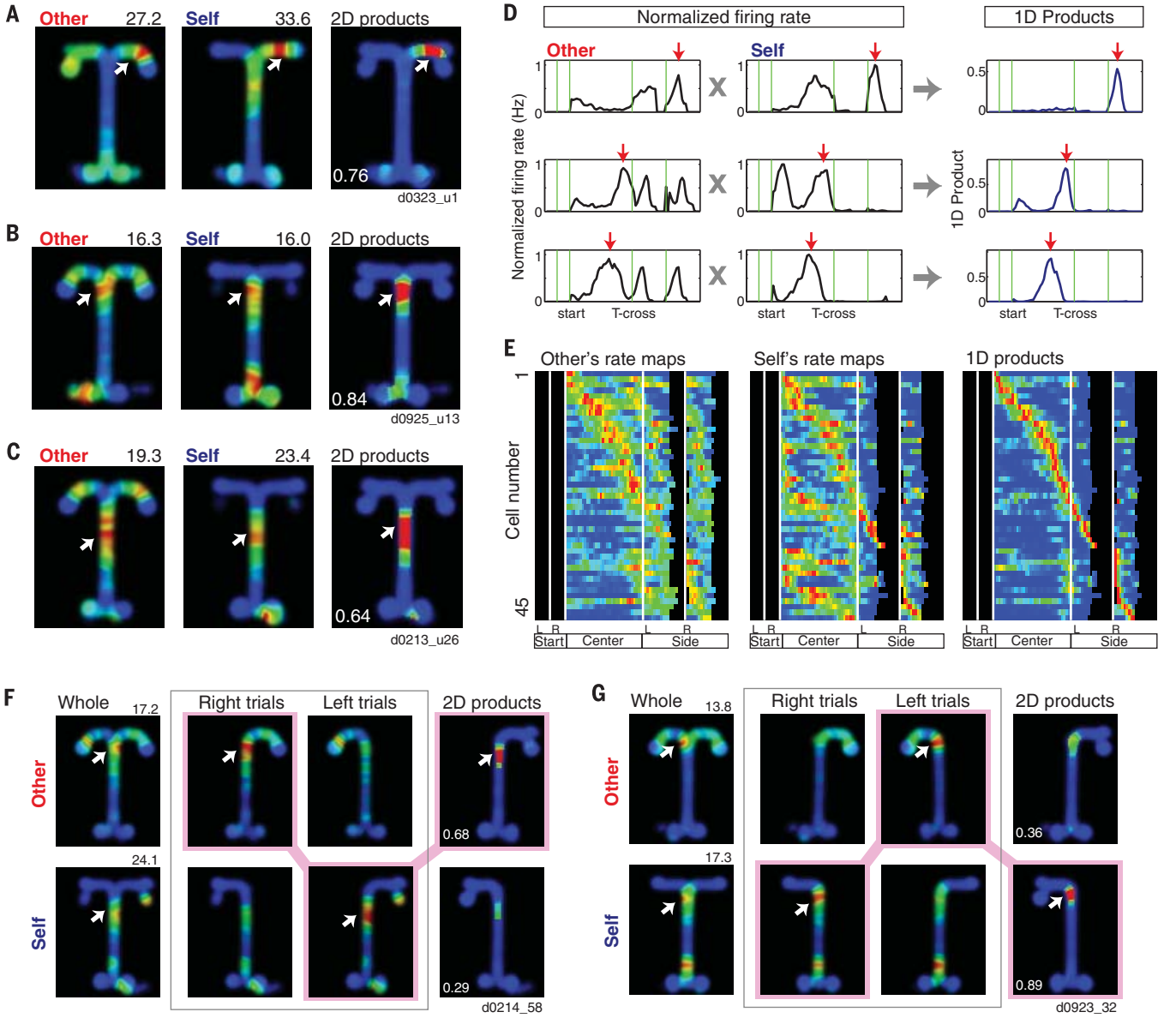

Fig. 3. Common place fields in self's and other's rate maps. (**A** to **C**) Common place fields of representative units in the other's (left) and the self's (middle) rate maps. (Right) The products (element-wise multiplications) of normalized other's and self's firing rates in each pixel. (**D**) Linearized other's (left) and self's (middle) firing rates and their products (right). The products are the element-wise multiplications of the normalized firing rates of the self and the other at each position, of the units shown in (A) to (C). This value was used to identify units with common place fields. (**E**) Linearized and normalized rate maps of units with common place fields aligned by the position with the maximum value of the products (n = 45 of 908 units). (**F** and **G**) Trajectory-specific common place fields of two representative units. (Left) Other's (top) and self's (bottom) rate maps of whole trials. (Middle) Rate maps with the left and right trials separated. (Right) The products of normalized other's and self's firing rates of right (top) and left (bottom) targeting trials in each pixel. Arrows indicate the centers of common place fields. The maximum color value of the product map was set as 0.5, and the values in the product map indicate the maximum of the product.

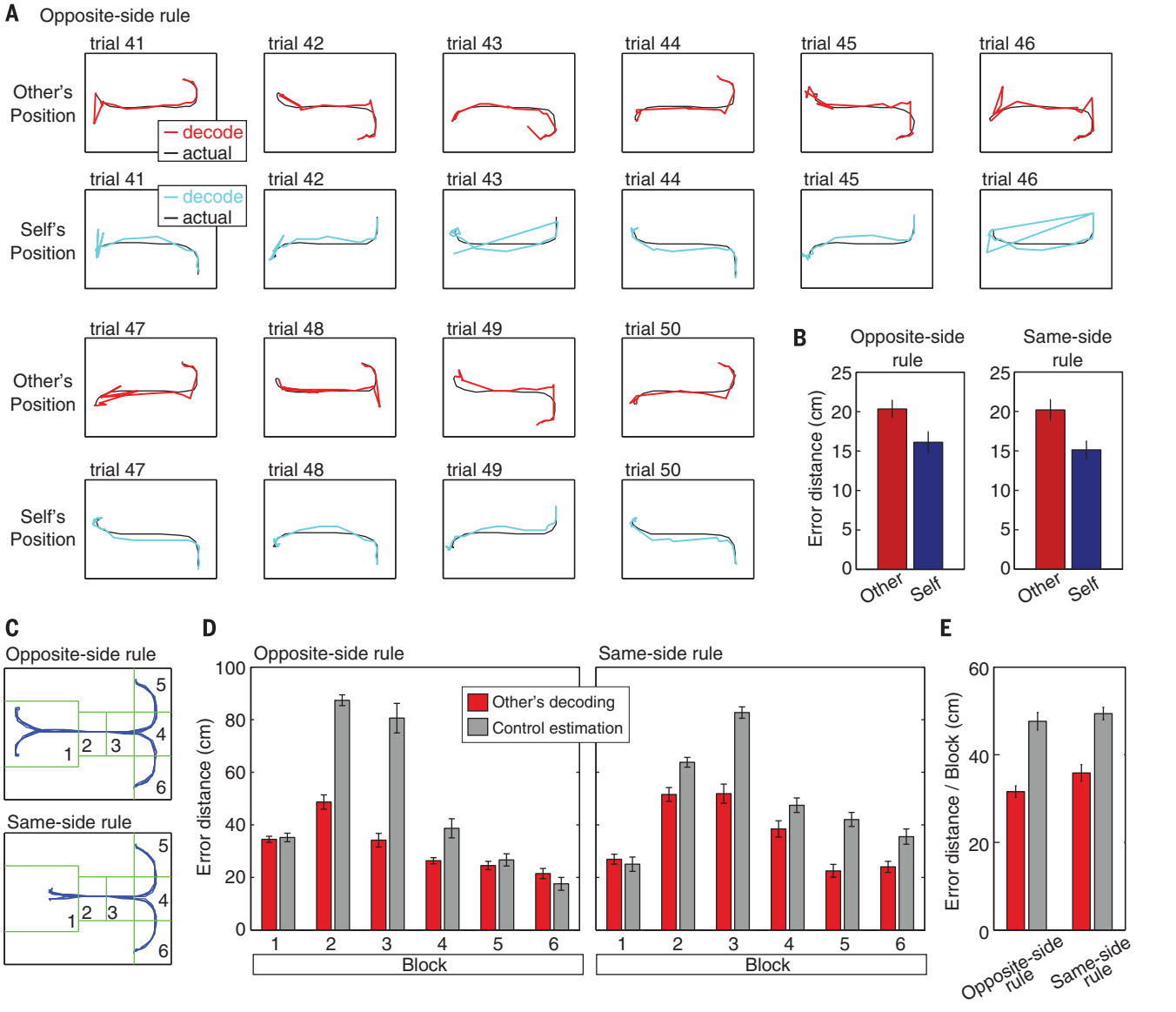

Fig. 4. Decoding other's and self's positions from spikes of hippocampal cells. (**A**) Reconstructed other's and self's positions in the opposite-side rule. Red and blue lines, reconstructed other's and self's positions, respectively. Black lines, actual trajectories of the other or self. (**B**) Mean error distances between actual and decoded positions (31 and 28 sessions from the opposite-side and same-side rules, respectively). (**C** to **E**) The reconstructions of other's positions by using prior templates calculated from trials including both rules. (C) Schematic of the division of other's trajectories into six blocks. (D) Error distances of reconstructed other's positions in each block. Red bars, distance between the actual and decoded other's positions. Gray bars, distance between the actual and estimated other's positions (n = 22 sessions) (two-way repeated measures analysis of variance: $P < 0.001$, $F_5 = 83.95$ for the opposite-side rule; $P < 0.001$, $F_5 = 72.6$ for the same-side rule). (E) Averaged error distances per block (two-tailed paired t test: $P < 0.001$, $t_{21} = -10.70$ for the opposite-side rule; $P < 0.001$, $t_{21} = -10.95$ for the same-side rule). Data are mean ± SEM.

REFERENCES AND NOTES

1. N. Burgess, E. A. Maguire, J. O'Keefe, *Neuron* **35**, 625–641 (2002).
2. A. D. Ekstrom *et al.*, *Nature* **425**, 184–188 (2003).
3. E. C. Tolman, *Psychol. Rev.* **55**, 189–208 (1948).
4. J. O'Keefe, L. Nadel, *The Hippocampus as a Cognitive Map* (Clarendon Press, Oxford, 1978).
5. G. Buzsáki, E. I. Moser, *Nat. Neurosci.* **16**, 130–138 (2013).
6. J. O'Keefe, J. Dostrovsky, *Brain Res.* **34**, 171–175 (1971).
7. E. R. Wood, P. A. Dudchenko, H. Eichenbaum, *Nature* **397**, 613–616 (1999).
8. I. Lee, D. Yoganarasimha, G. Rao, J. J. Knierim, *Nature* **430**, 456–459 (2004).
9. S. Leutgeb *et al.*, *Science* **309**, 619–623 (2005).
10. T. J. Wills, C. Lever, F. Cacucci, N. Burgess, J. O'Keefe, *Science* **308**, 873–876 (2005).
11. S. A. Ho *et al.*, *Neuroscience* **157**, 254–270 (2008).
12. S. S. Deshmukh, J. J. Knierim, *Hippocampus* **23**, 253–267 (2013).
13. X. Mou, D. Ji, *eLife* **5**, e18022 (2016).
14. J. S. Taube, R. U. Muller, J. B. Ranck Jr., *J. Neurosci.* **10**, 420–435 (1990).
15. T. Hafting, M. Fyhn, S. Molden, M. B. Moser, E. I. Moser, *Nature* **436**, 801–806 (2005).
16. D. J. Foster, M. A. Wilson, *Nature* **440**, 680–683 (2006).
17. P. Ravassard *et al.*, *Science* **340**, 1342–1346 (2013).
18. E. Kropff, J. E. Carmichael, M. B. Moser, E. I. Moser, *Nature* **523**, 419–424 (2015).
19. B. L. McNaughton, F. P. Battaglia, O. Jensen, E. I. Moser, M. B. Moser, *Nat. Rev. Neurosci.* **7**, 663–678 (2006).
20. S. Fujisawa, A. Amarasingham, M. T. Harrison, G. Buzsáki, *Nat. Neurosci.* **11**, 823–833 (2008).
21. J. O'Keefe, M. L. Recce, *Hippocampus* **3**, 317–330 (1993).
22. M. R. Mehta, A. K. Lee, M. A. Wilson, *Nature* **417**, 741–746 (2002).
23. G. Dragoi, G. Buzsáki, *Neuron* **50**, 145–157 (2006).
24. C. D. Harvey, F. Collman, D. A. Dombeck, D. W. Tank, *Nature* **461**, 941–946 (2009).

25. L. M. Frank, E. N. Brown, M. Wilson, *Neuron* **27**, 169–178 (2000).
26. E. R. Wood, P. A. Dudchenko, R. J. Robitsek, H. Eichenbaum, *Neuron* **27**, 623–633 (2000).
27. M. A. Wilson, B. L. McNaughton, *Science* **261**, 1055–1058 (1993).
28. K. Zhang, I. Ginzburg, B. L. McNaughton, T. J. Sejnowski, *J. Neurophysiol.* **79**, 1017–1044 (1998).
29. V. Gallese, L. Fadiga, L. Fogassi, G. Rizzolatti, *Brain* **119**, 593–609 (1996).
30. G. Rizzolatti, L. Craighero, *Annu. Rev. Neurosci.* **27**, 169–192 (2004).
31. S. Wirth *et al.*, *Science* **300**, 1578–1581 (2003).
32. R. Q. Quiroga, L. Reddy, G. Kreiman, C. Koch, I. Fried, *Nature* **435**, 1102–1107 (2005).
33. N. T. M. Robinson *et al.*, *Neuron* **94**, 677–688.e6 (2017).
34. F. L. Hitti, S. A. Siegelbaum, *Nature* **508**, 88–92 (2014).
35. T. Okuyama, T. Kitamura, D. S. Roy, S. Itohara, S. Tonegawa, *Science* **353**, 1536–1541 (2016).

ACKNOWLEDGMENTS

We thank A. Amarasingham for helpful suggestions on data analysis and T. J. McHugh and C. Yokoyama for comments on the manuscript. This work was supported by Japan Society for the Promotion of Science Grants-in-Aid for Scientific Research (KAKENHI) nos. 16K14561 and 16H01290 to T.D. and 15H05876 and 16H01519 to S.F. All data necessary to support the paper's conclusions are present in the paper and the supplementary materials.

SUPPLEMENTARY MATERIALS

www.sciencemag.org/content/359/6372/213/suppl/DC1
Materials and Methods
Figs. S1 to S13
Movies S1 and S2
References (*36*–*41*)

14 July 2017; accepted 7 December 2017
10.1126/science.aao3898

Spatial representations of self and other in the hippocampus

Teruko Danjo, Taro Toyoizumi and Shigeyoshi Fujisawa

Science **359** (6372), 213-218.
DOI: 10.1126/science.aao3898

The representation of others in space

Different sets of neurons encode the spatial position and orientation of an organism. However, social animals need to know the position of other individuals for social interactions, observational learning, and group navigation. Surprisingly, very little is known about how the position of other animals is represented in the brain. Danjo *et al.* and Omer *et al.* now report the discovery of a subgroup of neurons in hippocampal area CA1 that encodes the presence of conspecifics in rat and bat brains, respectively.

Science, this issue p. 213, p. 218